RSC Advances

PAPER

View Article Online
View Journal | View Issue



Cite this: *RSC Adv.*, 2018, **8**, 2449

# Self-radiolysis of tritiated water. 4. The scavenging effect of azide ions ($N_3^-$) on the molecular hydrogen yield in the radiolysis of water by $^{60}$Co γ-rays and tritium β-particles at room temperature

Sunuchakan Sanguanmith,[a] Jintana Meesungnoen,[a] Craig R. Stuart,[b] Patrick Causey[c] and Jean-Paul Jay-Gerin *[a]

The effect of the azide ion $N_3^-$ on the yield of molecular hydrogen in water irradiated with $^{60}$Co γ-rays (~1 MeV Compton electrons) and tritium β-electrons (mean electron energy of ~7.8 keV) at 25 °C is investigated using Monte Carlo track chemistry simulations in conjunction with available experimental data. $N_3^-$ is shown to interfere with the formation of $H_2$ through its high reactivity towards hydrogen atoms and, but to a lesser extent, hydrated electrons, the two major radiolytic precursors of the $H_2$ yield in the diffusing radiation tracks. Chemical changes are observed in the $H_2$ scavengeability depending on the particular type of radiation considered. These changes can readily be explained on the basis of differences in the initial spatial distribution of primary radiolytic species (*i.e.*, the structure of the electron tracks). In the "short-track" geometry of the higher "linear energy transfer" (LET) tritium β-electrons (mean LET ~5.9 eV nm$^{-1}$), radicals are formed locally in much higher initial concentration than in the isolated "spurs" of the energetic Compton electrons (LET ~0.3 eV nm$^{-1}$) generated by the cobalt-60 γ-rays. As a result, the short-track geometry favors radical–radical reactions involving hydrated electrons and hydrogen atoms, leading to a clear increase in the yield of $H_2$ for tritium β-electrons compared to $^{60}$Co γ-rays. These changes in the scavengeability of $H_2$ in passing from tritium β-radiolysis to γ-radiolysis are in good agreement with experimental data, lending strong support to the picture of tritium β-radiolysis mainly driven by the chemical action of short tracks of high local LET. At high $N_3^-$ concentrations (>1 M), our $H_2$ yield results for $^{60}$Co γ-radiolysis are also consistent with previous Monte Carlo simulations that suggested the necessity of including the capture of the precursors to the hydrated electrons (*i.e.*, the short-lived "dry" electrons prior to hydration) by $N_3^-$. These processes tend to reduce significantly the yields of $H_2$, as is observed experimentally. However, this dry electron scavenging at high azide concentrations is not seen in the higher-LET $^3$H β-radiolysis, leading us to conclude that the increased amount of intra-track chemistry intervening at early time under these conditions favors the recombination of these electrons with their parent water cations at the expense of their scavenging by $N_3^-$.

Received 13th November 2017
Accepted 22nd December 2017

DOI: 10.1039/c7ra12397c

rsc.li/rsc-advances



## 1. Introduction

A detailed understanding of the radiolysis of water and aqueous solutions is important both from a fundamental science point of view and for a variety of practical applications,[1–4] in particular, in the nuclear power industry and in radiation biology where living cells and tissues consist mainly of water (~70–85% by weight). Exposed to ionizing radiation, water is the site of ionizations and excitations:

$$H_2O \rightsquigarrow H_2O^{\bullet+} + e^- \text{ (ionization)}$$

$$H_2O \rightsquigarrow H_2O^* \text{ (excitation)},$$

which result, within a few picoseconds, in a cascade of events leading to the formation of free radicals and molecular products along the track of the incident radiation. Ejected secondary electrons (also called "dry" electrons) have generally sufficient kinetic energy to cause further ionizations and excitations in close proximity to the original water positive ion. After slowing down to sub-excitation energies and thermalization, these electrons become trapped and hydrated. Under ordinary irradiation conditions (*i.e.*, at modest dose rates so that no track

[a]*Département de médecine nucléaire et de radiobiologie, Faculté de médecine et des sciences de la santé, Université de Sherbrooke, 3001, 12e Avenue Nord, Sherbrooke, Québec, J1H 5N4, Canada. E-mail: jean-paul.jay-gerin@USherbrooke.ca*

[b]*Reactor Chemistry and Corrosion Branch, Canadian Nuclear Laboratories, Chalk River, Ontario, K0J 1J0, Canada*

[c]*Radiological Protection Research and Instrumentation Branch, Canadian Nuclear Laboratories, Chalk River, Ontario, K0J 1J0, Canada*

overlap occurs), the initial products of radiolysis are generated in a highly nonhomogeneous "track structure" geometry.[5–11] They include[12,13] the hydrated electron ($e_{aq}^-$), $H_3O^+$, $OH^-$, $H^\bullet$, $H_2$, $^\bullet OH$, $H_2O_2$, $O_2^{\bullet-}$ (or its protonated form $HO_2^\bullet$; p$K_a$ = 4.8 at 25 °C), $O(^1D)$, $^\bullet O^\bullet(^3P)$, $O^{\bullet-}$, *etc.* This early nonhomogeneous spatial distribution of radiolytic species is strongly dependent on the radiation quality, a measure of which is given by the "linear energy transfer" (LET) (also called "stopping power" by physicists and denoted by $-dE/dx$). For low-LET, sparsely ionizing radiation (such as γ-rays from $^{60}$Co or fast electrons; LET ~0.3 eV nm$^{-1}$), tracks are formed initially by widely spaced clusters of reactive species, commonly known as "spurs" (spherical in shape).[14,15] In this case, the predominant effect of radiolysis is radical production. In fact, when diffusion has brought about homogeneity in the system (*i.e.*, within a few microseconds after the initial energy deposition), relatively few radicals have combined in the spurs, resulting in an excess of radicals over molecular products. However, with increasing LET, the isolated spur structure changes to a situation in which the spurs eventually overlap and form (initially) a dense continuous column of species. This is actually the case for the low-energy β-electrons of tritium, which are involved in the "self-radiolysis" of tritiated water ($^3$HOH),[16–18] the subject matter of the present study. In the terminology of the Mozumder–Magee model of energy deposition,[6,19] while the Compton electrons (~1 MeV) produced by $^{60}$Co γ-radiolysis predominantly form spurs, these soft, higher-LET tritium β-electrons predominantly deposit their energy as "short tracks". This leads to an increased local concentration of reactants and therefore an increased amount of intra-track chemistry that favors radical–radical reactions. Under these conditions, the radiation chemical yields (or *G*-values)[20] of the molecular products increase at the expense of the individual radicals. For the sake of illustration, Fig. 1 shows typical 2-D representations of the complete track of a 7.8 keV $^3$H β-electron and the track segment of a 300 MeV proton (which mimics irradiation with $^{60}$Co γ-rays), calculated with our IONLYS Monte Carlo track structure simulation code (see below).

In close connection with the LET and the relationship between track structure and chemistry, one critical area of research focuses on elucidating the basic radiation chemical mechanisms that operate in the "self-radiolysis" of tritiated water as compared with $^{60}$Co γ-radiolysis.[21–26] The present paper is the fourth in a series[18,27,28] dedicated to this subject. The Monte Carlo track-chemistry simulation work we reported previously revealed significant differences between the chemical properties of short tracks and spurs using either γ-rays/fast electrons or tritium β-particles. Overall, the results of our simulations provided strong support for the picture of tritium β-radiolysis mainly driven by the chemical action of short tracks of high local LET. In the present study, we now attempt to distinguish further the chemical properties of spur and short track geometries by examining the differences in the scavengeability of molecular $H_2$ – whose yields are relatively well-documented experimentally[21,22,25,26,29–32] – when passing from γ- to tritium β-electron radiolysis.

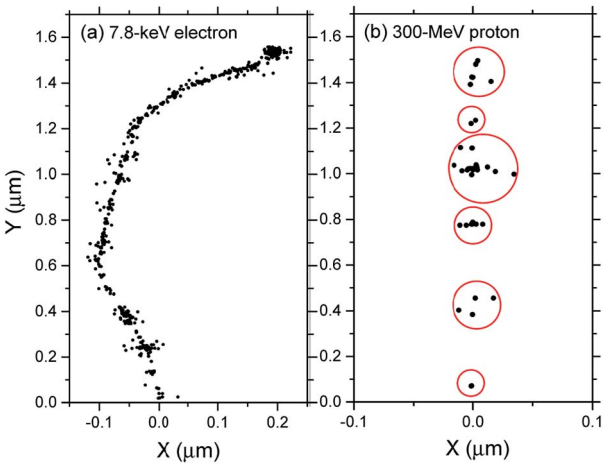


Fig. 1 Simulated track histories (projected into the *XY* plane of figure) of a 7.8 keV tritium β-electron (complete track; mean LET ~ 5.9 eV nm$^{-1}$) (panel a) and a 300 MeV proton (track segment; LET ~ 0.3 eV nm$^{-1}$) (panel b) incident in liquid water at 25 °C. The two irradiating particles are generated at the origin and start traveling along the *Y* axis. Dots represent the energy deposited at points where an interaction occurred.

Molecular hydrogen is one of the most interesting radiolytic species, in part because of the questions it raises about the source of its formation. At very short times (<50–300 fs) after the passage of the ionizing radiation,[33] $H_2$ can be formed by the following reactions:[34,35]

(1) geminate recombination of the sub-excitation electron ($e_{sub}^-$)[36] with its parent cation $H_2O^{\bullet+}$

$$H_2O^{\bullet+} + e_{sub}^- \rightarrow H_2O^*$$

(2) "dissociative electron attachment" (or DEA) involving the resonant capture of $e_{sub}^-$ by a water molecule

$$H_2O + e_{sub}^- \rightarrow (H_2O^{\bullet-*}) \rightarrow H^- + {}^\bullet OH,$$

followed by

$$H^- + H_2O \rightarrow H_2 + OH^-$$

(3) dissociation of excited water molecules (formed either by direct excitation or by geminate electron-hole recombination)

$$H_2O^* \rightarrow H_2 + O(^1D),$$

where $O(^1D)$ is the oxygen atom in its singlet $^1$D first excited state.

In the low-LET γ-irradiation case, this "initial" – then described as "unscavengeable" (*i.e.*, not removable by scavenger experiments) – $H_2$ yield was first estimated by Schwarz[37] in 1969 to be ~30% of the total "escape" yield[20] for molecular hydrogen [$g(H_2)$ = 0.45 molecule/100 eV].[5,7,11,12] Recent scavenger studies[38] have shown, however, that Schwarz's initial estimate was

 

undervalued. In fact, it was found that a major fraction (~75%, *i.e.*, ~0.34 molecule/100 eV) of the total $H_2$ produced was due to reactions of the dry/subexcitation electrons in the subpicosecond physicochemical stage of the radiolysis. In other words, these results suggest that only ~0.11 molecule of $H_2$ per 100 eV remains to be formed during the subsequent nonhomogeneous chemical stage (*i.e.*, in the radiation tracks as they expand by diffusion) on the picosecond–microsecond time scale. At this stage, three radical–radical combination reactions of the hydrated electron and $H^\bullet$ atom intervene in hydrogen formation. They are[18,34,39,40]

$$e_{aq}^- + H^\bullet (+H_2O) \rightarrow H_2 + OH^-, k_1 = 2.5 \times 10^{10}\ M^{-1}\ s^{-1} \quad (1)$$

$$e_{aq}^- + e_{aq}^- (+2H_2O) \rightarrow H_2 + 2OH^-, k_2 = 6.2 \times 10^{9}\ M^{-1}\ s^{-1} \quad (2)$$

and, but to a much lesser extent,

$$H^\bullet + H^\bullet \rightarrow H_2, k_3 = 4.6 \times 10^{9}\ M^{-1}\ s^{-1} \quad (3)$$

with the corresponding rate constants ($k$) taken from the compilation of Elliot and Bartels.[12]

Besides the mechanism of its formation, a better knowledge of the radiolytic production of molecular hydrogen is crucial in the "water chemistry" management of current water-cooled nuclear reactors to optimize plant performance and lifetime. As we know,[2] $H_2$ is currently added to the primary coolant water to suppress the formation of stable oxidizing products ($H_2O_2$ and eventually its decomposition product $O_2$) from water radiolysis by a short chain reaction, thereby preventing corrosion and activity transport. The *in situ* radiolytic formation of $H_2$ in these reactors could, therefore, affect the minimum concentration of excess $H_2$, referred to as the "critical hydrogen concentration",[41,42] required to suppress net radiolysis (no stable products formed) in the cores. Knowledge of this optimum $H_2$ level, which would minimize the damaging consequences of corrosion, is still a subject of debate in the chemical literature.

The anomalous increase in the escape yield of $H_2$ at high temperature is another key motivation for this study. In fact, although $H_2$ is a molecular product, $g(H_2)$ increases with temperature under γ/fast electron irradiation,[12,34,35] from ~0.45 molecule/100 eV at 25 °C to ~0.76 molecule/100 eV at 350 °C. This behavior is an exception to the generally accepted diffusion-kinetic model,[6,43] which predicts that, when the temperature increases, diffusion of free radicals out of spurs or tracks becomes more important than recombination, resulting in less molecular recombination products. At present, no definitive mechanism has yet been established to account for this anomalous radiolytic production of $H_2$ at high temperature.[34]

For these different reasons, the escape yield of $H_2$ has attracted much attention from experimentalists and modelers in order to explore in more detail its formation under various irradiation conditions. In this work, we use Monte Carlo track chemistry simulations to examine further the chemical differences underlying the production of molecular hydrogen in tritium β-radiolysis as compared with cobalt γ-radiolysis. No real-time studies on $H_2$ formation have been performed; its temporal dependence is usually probed by varying the concentration of appropriate scavengers for the hydrated electron and the hydrogen atom, which are the dominant free radical precursors of $H_2$ within the diffusing spurs or tracks. We here report data on the scavengeability by azide ions ($N_3^-$) of the molecular $H_2$ yield produced by γ- and tritium β-radiolysis. This particular scavenger was chosen as it presents very different reactivities towards $e_{aq}^-$ and $H^\bullet$ atoms, being highly unreactive towards the former but reacting very rapidly with the latter. Our aim is to study the different $H_2$ scavengeabilities found for the two types of irradiation considered and to examine how these differences reflect the structure of the radiation track (*i.e.*, spurs *vs.* short tracks) in both cases.

## 2. Monte-Carlo track chemistry simulations

Monte Carlo simulation methods are well suited to take into account the stochastic nature of the complex sequence of events that are generated in irradiated aqueous solutions containing reactive scavengers. In the case of interest here, the experimentally observed yield value for molecular hydrogen is a composite one to which each of the processes producing $H_2$ contributes. The addition of a scavenger that competes with these processes to different extents will change the relative amount that each process contributes to the total yield. The simulation allows the reconstruction of the intricate action of the radiation, thus providing a powerful tool for studying the relationship between the initial radiation track structure, the ensuing chemical processes, and the stable final products formed. In this work, a full Monte Carlo track-chemistry computer code, called IONLYS-IRT,[11] has been used to simulate the radiolysis of water and aqueous solutions containing various concentrations of scavengers. This code first models, in a 3D geometrical environment, the initial, highly nonhomogeneous radiation track structure ("IONLYS" program), and then the diffusion and chemical reactions of the various radical and molecular products formed by radiolysis with themselves or with solutes if present ("IRT" program). A detailed description of this code has been given previously.[11,18,28,34,44–46] Only a brief overview of its most essential features is given below.

The IONLYS code is a step-by-step simulation program that covers the early physical and physicochemical stages[47] of radiation action up to ~1 ps in the track development. It is composed of two modules. One is for transporting the investigated incident charged particle (called either TRACEPR for an impacting primary electron or TRACPRO/TRACION for an incident proton/ion). The other (called TRACELE) is for transporting all of the energetic (or dry) electrons (collectively named "secondary electrons") resulting from the ionization of the water molecules until they become hydrated. In this study, we used the TRACEPR module of IONLYS to simulate the track structures of low-energy (~7.8 keV) tritium β-electrons. As for

the TRACPRO module, it was used here to simulate track segments of 300 MeV incident protons (which, as mentioned before, mimic $^{60}$Co γ/fast electron irradiation) (see Fig. 1).

The complex, highly nonhomogeneous spatial distribution of reactants at the end of the physicochemical stage is provided as an output of the IONLYS (TRACELE) program. It is then used directly as the starting point for the subsequent nonhomogeneous chemical stage[47] (from ∼1 ps to ∼0.1–1 μs at 25 °C,[48] *i.e.*, until all tracks/spurs have dissipated). This stage, during which all different species diffuse (we assume ∼1 ps also marks the beginning of diffusion) randomly at rates determined by their diffusion coefficients and react with one another or with any added solutes present at the time of irradiation, is covered by our "independent reaction times" (IRT) program. This program employs the IRT method,[49,50] a computer-efficient stochastic simulation technique used to simulate reaction times without having to follow the trajectories of the diffusing species. Its implementation has been previously described in detail[45] and its ability to give accurate, time-dependent chemical yields has been well validated[51,52] by comparison with full random flight (or step-by-step) Monte Carlo simulations, which do follow the reactant trajectories in detail. Finally, this IRT program has also been used successfully to describe the evolution of radiation-induced yields in the homogeneous chemical stage[47] after spur/track expansion is complete (*i.e.*, when the radiolytic products become homogeneously distributed in the bulk solution), in the time domain typically beyond a few microseconds.

The reaction scheme and rate constants for the radiolysis of pure liquid water at 25 °C employed in the current version of IONLYS-IRT are the same as used previously (see Table 1 of ref. 18). The values of the diffusion coefficients of the various intervening track species are listed in Table 6 of ref. 53. In order to simulate the radiolysis of the $N_3^-$ solutions, we have supplemented the pure-water reaction scheme to include the primary $e_{aq}^-$ and $H^\bullet$ atom scavenging reactions that occur in the system (*vide infra*). Under normal irradiation conditions, the concentrations of radiolytic products are low compared with the background concentrations of $N_3^-$ ions considered, and their reactions could be modeled in the IRT program as pseudo first-order reactions. In the computer simulations reported here, the diffusion coefficient used for $N_3^-$ in liquid water at 25 °C was $1.84 \times 10^{-5}$ cm$^2$ s$^{-1}$.[54] This same value was also used for the diffusion coefficient of the azide radical $N_3^\bullet$.

In addition, we have introduced in the IRT program the effect of the ionic strength of the solutions on all reactions between ions.[55] The correction to the reaction rate constants was made as described in ref. 56 and 57. Finally, for highly concentrated $N_3^-$ solutions (some experimental data are available up to 5 M), we neglected complications due the "direct" action of ionizing radiation on the solute (which our Monte Carlo code does not take into account). This is certainly a very good approximation for ∼1–2 M $N_3^-$ concentrations (in that case, ∼2–4% of the total energy is absorbed directly by the azide anions). For 5 M $N_3^-$ solutions, the proportion of direct effects increases to about 11%, which remains relatively low and may reasonably still be ignored at least as a first approximation.

To mimic the effects of $^{60}$Co γ/fast electron-radiolysis, we used short segments (typically, ∼150 μm) of ∼300 MeV irradiating proton tracks, over which the average LET of the proton remains nearly constant and equal to ∼0.3 eV nm$^{-1}$ at 25 °C.[2,45] Such model calculations thus gave "track segment" yields[8,45] at a well-defined LET. Briefly, the simulations, performed with the TRACPRO module of IONLYS, consisted of following the transport and energy loss of an incident proton until it penetrated the chosen length of the track segment into the solution. As shown in Fig. 1, due to its large mass, the impacting proton is almost not deflected by collisions with the target electrons. The number of individual proton "histories" (usually ∼150) was chosen to ensure only small statistical fluctuations in the computed averages of chemical yields, while keeping acceptable computer time limits.

As indicated above, tritium-β primary electron track structures were simulated using the TRACEPR module of IONLYS. Each simulation typically involved 6000 different whole track histories. This number was chosen to permit averaging of results with acceptable statistical confidence. In all the simulations, a single "effective" initial electron energy of ∼7.8 keV (mean LET in water: ∼5.9 eV nm$^{-1}$)[16] was used to mimic the radiation chemical action of the tritium β-particles at 25 °C (Fig. 1). This energy was found previously to be better suited to produce representative *G*-values when using tritium β-rays than the commonly used mean kinetic energy of ∼5.7 keV released by tritium decay.[18,58]

Throughout this study, we assumed that tritiated water could simply be described as a "dilute" solution of $^3$HOH in light water, with concentrations of low volumic activity (typically, less than ∼1 Ci per mL) so that dose-rate effects could be ignored.[25,59]

## 3. Results and discussion

The azide ion $N_3^-$ reacts very fast with $H^\bullet$ atoms and very slowly with the hydrated electron, according to[22,25,60–63]

$$N_3^- + H^\bullet \rightarrow HN_3^{\bullet-},\ k_4 = 3.15 \times 10^9\ M^{-1}\ s^{-1} \quad (4)$$

$$N_3^- + e_{aq}^- \rightarrow \text{products},\ k_5 \leq 1.5 \times 10^6\ M^{-1}\ s^{-1}, \quad (5)$$

where the decay of $HN_3^{\bullet-}$ by proton addition has been shown not to involve $H_2$ as a final product[63] and where it is assumed here that the products of reaction (5) do not influence the $H_2$ chemistry. In contrast, its protonated form, hydrazoic acid (or hydrogen azide) $HN_3$,[22,54,63]

$$N_3^- + H^+ \leftrightarrow HN_3,\ pK_a(HN_3/N_3^-) = 4.7 \text{ in water at } 25\ ^\circ C,\ k_6(\text{forward}) \approx 10^9\text{–}10^{10}\ M^{-1}\ s^{-1}, \quad (6)$$

is highly reactive towards $e_{aq}^-$ but it reacts slower with $H^\bullet$ atoms:[60,62–64]

$$HN_3 + e_{aq}^- \rightarrow HN_3^{\bullet-},\ k_7 = 1.2 \times 10^{10}\ M^{-1}\ s^{-1} \quad (7)$$

$$HN_3 + H^\bullet \rightarrow \text{products} (\neq H_2),\ k_8 = 6.3 \times 10^7\ M^{-1}\ s^{-1} \quad (8)$$

 

However, even if a fraction of the azide ions may react with $H^+$ ions in the spurs/tracks[13,22] to yield $HN_3$, especially at high $N_3^-$ concentration (which is equivalent to short times), the Henderson–Hasselbalch equation indicates that, under the neutral pH conditions of this work, this compound will exist almost entirely in anion form. Hence, $HN_3$ should not significantly affect the radiolytic $H_2$ yield.

The azide ion can also react with the $^{\bullet}OH$ radical to produce the one-electron oxidant azide radical, $N_3^{\bullet}$:[64,65]

$$N_3^- + {}^{\bullet}OH \rightarrow N_3^{\bullet} + OH^-,\ k_9 = 1.2 \times 10^{10}\ M^{-1}\ s^{-1}, \quad (9)$$

or, for its protonated form,[64]

$$HN_3 + {}^{\bullet}OH \rightarrow N_3^{\bullet} + H_2O,\ k_{10} < 10^7\ M^{-1}\ s^{-1}. \quad (10)$$

In this case, the $^{\bullet}OH$ radicals (or at least part of them) are replaced by the $N_3^{\bullet}$ radicals and we need to consider the following reactions:[60,62,64,66–71]

$$N_3^{\bullet} + e_{aq}^- \rightarrow N_3^-,\ k_{11} = 2.4 \times 10^{10}\ M^{-1}\ s^{-1} \quad (11)$$

$$N_3^{\bullet} + H^{\bullet} \rightarrow HN_3,\ k_{12} \approx 10^{10}\ M^{-1}\ s^{-1} \quad (12)$$

$$N_3^{\bullet} + H_2O_2 \rightarrow \text{products},\ k_{13} < 5 \times 10^6\ M^{-1}\ s^{-1} \quad (13)$$

$$N_3^{\bullet} + N_3^{\bullet} \rightarrow 3N_2,\ k_{14} = 3.9 \times 10^9\ M^{-1}\ s^{-1} \quad (14)$$

$$N_3^{\bullet} + N_3^- \rightarrow (N_3)_2^{\bullet -},\ k_{15} = 2.4 \times 10^5\ M^{-1}\ s^{-1} \quad (15)$$

The rather slow reaction of azide with $e_{aq}^-$ virtually excludes any effect of $N_3^-$ on reactions involving $e_{aq}^-$ in the spurs/tracks,[60] particularly in solutions with low $N_3^-$ concentration. Indeed, even in a 5 M $N_3^-$ solution, the scavenging time[72] of $e_{aq}^-$ by $N_3^-$ is about the same order of magnitude as the lifetime of a spur (~0.2 μs)[48] in the $^{60}$Co γ-radiolysis of water at 25 °C. Under these conditions, the molecular hydrogen yield was measured in irradiated *aerated* azide solutions.[22,25,60] Oxygen between ~$2.5 \times 10^{-4}$ M (air-saturated conditions) and ~$3–5 \times 10^{-5}$ M was used as $e_{aq}^-$ scavenger on the ~0.1–1 μs time scale. Noteworthy, the azide radical is inert towards molecular oxygen,[66] but may react with the superoxide anion radical[62,66]

$$N_3^{\bullet} + O_2^{\bullet -} \rightarrow O_2 + N_3^-,\ k_{16} = 1.2 \times 10^{10}\ M^{-1}\ s^{-1}. \quad (16)$$

While these low $O_2$ concentrations hardly affect $g(H_2)$, they do prevent, at long times, the reactions of $e_{aq}^-$ with itself and with water[62]

$$e_{aq}^- + H_2O \rightarrow H^{\bullet} + OH^-,\ k_{17} = 19\ M^{-1}\ s^{-1} \quad (17)$$

in the bulk of the solutions.

Fig. 2 (panels a and b) shows the effect of azide concentration on the kinetics of $H_2$ formation over the interval ~1 ps to 10 μs, as obtained from our Monte Carlo simulations of the radiolysis of aerated neutral pH aqueous solutions of $NaN_3$ by ~300 MeV incident protons and ~7.8 keV tritium β-electrons at 25 °C. Results are shown for six different concentrations of azide anions, ranging from $10^{-4}$ to 5 M. As can be seen, for both types of radiation, the time profiles of the $H_2$ yields are essentially similar although the magnitude of the $G(H_2)$ values differs. In fact, the simulations show a clear increase in the absolute value of $G(H_2)$ for $^3$H β-electrons compared to $^{60}$Co γ-rays. As mentioned earlier, this increase in $H_2$ yields, when comparing the effects of higher-LET tritium β-radiolysis with the γ/fast electron-radiolysis, is consistent with differences in the initial structure of electron tracks in the two cases. In the short-track geometry of the β-electrons (in contrast with spur geometry),

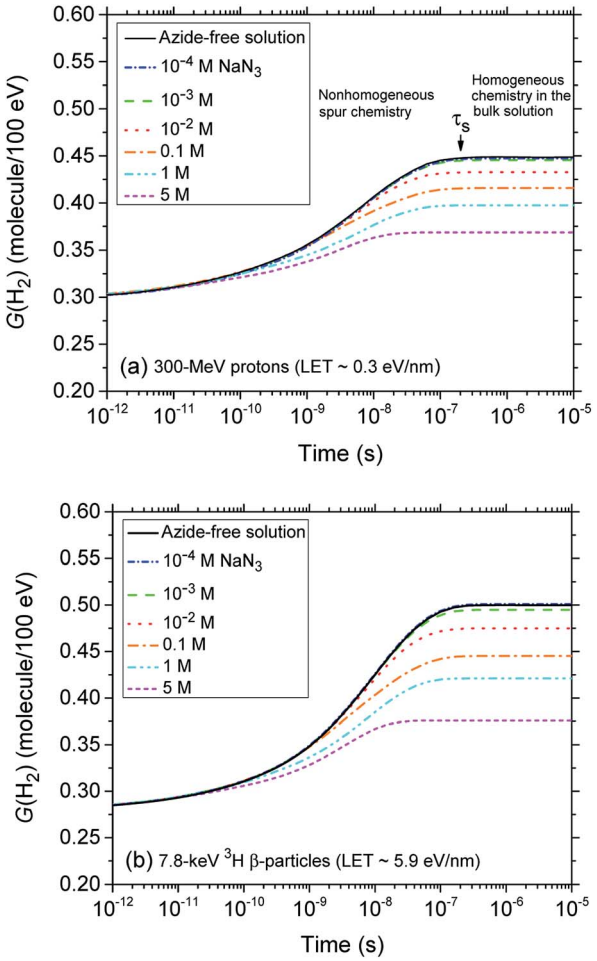


Fig. 2 Time evolution of the $H_2$ yield (in molecule per 100 eV) for the radiolysis of air-saturated aqueous sodium azide ($NaN_3$) solutions by 300 MeV incident protons (which mimic irradiation with $^{60}$Co γ-rays or fast electrons, LET ~0.3 eV nm$^{-1}$) (panel a) and by 7.8 keV $^3$H β-particles (LET ~5.9 eV nm$^{-1}$) (panel b) at neutral pH and 25 °C. Calculations were carried out using our Monte-Carlo track chemistry simulations over the time interval 1 ps to 10 μs. The blue, green, red, orange, cyan, and magenta lines correspond to six different concentrations of $N_3^-$ anions: $10^{-4}$, $10^{-3}$, $10^{-2}$, 0.1, 1, and 5 M, respectively. For both types of radiation, the limiting plateau values of $G(H_2)$ continuously decrease with increasing the concentration of $N_3^-$ ions. For $^{60}$Co γ/fast electron irradiation, the arrow pointing downwards indicates the time $\tau_s$ ~0.2 μs required for the changeover from nonhomogeneous spur kinetics to homogeneous kinetics in the bulk solutions, at 25 °C. The black solid line in panels a and b show the kinetics of $H_2$ formation in azide-free aerated solutions (shown here for the sake of reference). Finally, the concentration of dissolved oxygen used in the simulations was $2.5 \times 10^{-4}$ M.

the reactive intermediates are formed in much closer initial proximity, which is favorable to the additional formation of $H_2$ through the inter-radical combination reactions (1)–(3).

The decrease in the yield of $H_2$ with concentration of $N_3^-$ ions for 300 MeV incident protons and 7.8 keV $^3$H β-electrons in the radiolysis of aerated azide solutions is further illustrated in Fig. 3. The $H_2$ yields shown in this figure are the $G(H_2)$ limiting plateau values corresponding to each considered $N_3^-$ concentration, taken from Fig. 2. As can be seen, our simulated yields compare well with the experimental escape yields of Gagnon and Appleby,[22] Christman,[25] and Peled *et al.*[60] obtained for $^{60}$Co γ and tritium β-particle irradiations. In the case of γ-radiolysis, this agreement is particularly good at low and moderated $N_3^-$ concentrations. However, at concentrations higher than ~0.5 M, there are significant differences, the experimentally observed $H_2$ yields showing a very sharp decrease[73] compared to the simulation results. This efficiency in reducing the molecular hydrogen produced strongly suggests that the concentration of azide ions is now high enough to allow their reaction with the dry electron ($e_{dry}^-$) prior to trapping and hydration (*i.e.*, with the precursor to $e_{aq}^-$), in the subpicosecond physicochemical stage.[33]

Similar findings about the $N_3^-$ scavenging of the short-lived hydrated electron precursor were obtained by Harris and Pimblott[26] in recent Monte Carlo studies of the $^{60}$Co γ-radiolysis of azide solutions of concentration greater than 1 M. The present study clearly corroborates their results. Assuming the validity of

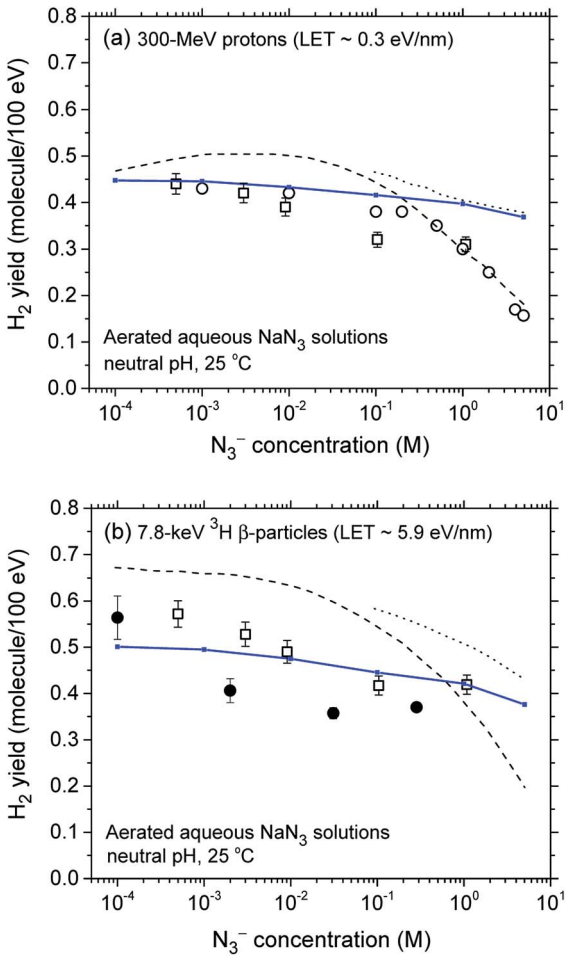


Fig. 3 Decrease in the molecular hydrogen yield (in molecule per 100 eV) with concentration of $N_3^-$ ions for 300 MeV incident protons (LET ~ 0.3 eV nm$^{-1}$) (panel a) and for 7.8 keV $^3$H β-particles (LET ~ 5.9 eV nm$^{-1}$) (panel b) in the radiolysis of air-saturated aqueous azide ($NaN_3$) solutions (neutral pH, 25 °C), calculated from our Monte Carlo simulations over the range of $10^{-4}$ to 5 M. The blue solid lines show our simulated results (see text). Experimental data for γ and tritium β-particle irradiations: (●), ref. 22; (□), ref. 25; (○), ref. 60. For the sake of comparison, the $H_2$ yields calculated from ref. 26 for both types of radiation, assuming that $N_3^-$ scavenges the short-lived precursor to $H_2$ with a rate constant of $10^{12}$ M$^{-1}$ s$^{-1}$ (dashed line) and does not scavenge the short-lived precursor to $H_2$ (dotted line), are also shown in the figure.

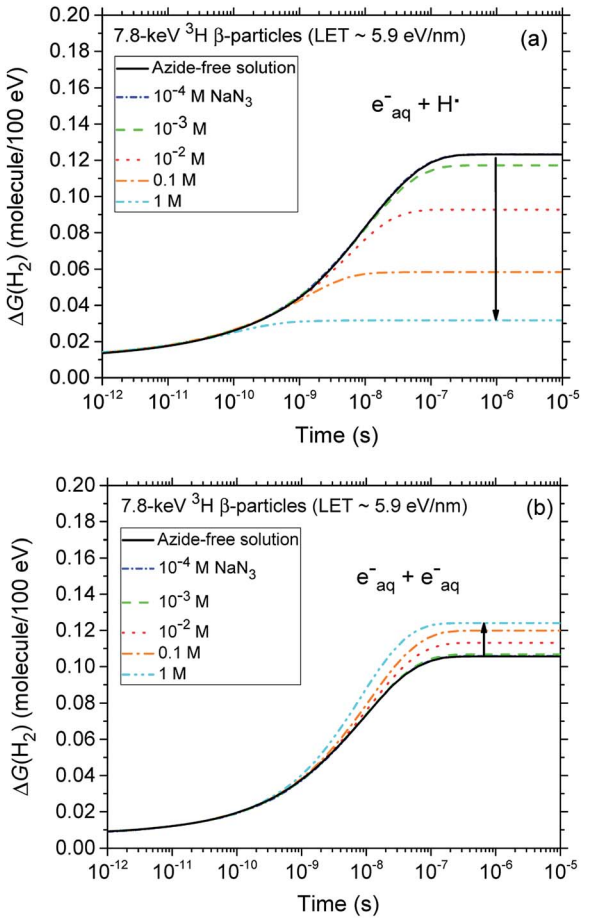


Fig. 4 Time dependence of the extents $\Delta G(H_2)$ (in molecule/100 eV) of the reactions ($e_{aq}^-$ + H•) (panel a) and ($e_{aq}^-$ + $e_{aq}^-$) (panel b) that contribute to the formation of molecular hydrogen, calculated from our Monte Carlo simulations of the radiolysis of air-saturated aqueous azide ($NaN_3$) solutions (pH neutral, 25 °C) by 7.8 keV $^3$H β-particles (LET ~ 5.9 eV nm$^{-1}$) in the time interval 1 ps to 10 μs. The blue, green, red, orange, and cyan lines correspond to the five different concentrations of azide anions studied: $10^{-4}$, $10^{-3}$, $10^{-2}$, 0.1, and 1 M, respectively (see text). For the sake of reference, the black lines in panels a and b show the cumulative yield variations $\Delta G(H_2)$ of the two reactions ($e_{aq}^-$ + H•) and ($e_{aq}^-$ + $e_{aq}^-$) that contribute to the formation of $H_2$ in azide-free solutions. Finally, the concentration of dissolved oxygen used in the simulations was 2.5 × $10^{-4}$ M.

this hypothesis would imply a ($e_{dry}^-$ + $N_3^-$) reaction rate constant of $\sim 10^{12}$–$10^{13}$ $M^{-1}$ $s^{-1}$ at 25 °C, in agreement with Harris and Pimblott[26,74] results.

For the case of $^3$H β-particle radiolysis, the effectiveness in lowering $g(H_2)$ at high azide concentration differs considerably from the case of γ-radiolysis. Despite a relatively large dispersion of experimental data,[75] we do not observe any sharp decrease at concentrations higher than ~0.1–1 M as we do for γ irradiation. There is only a slight continuous decrease of the yield of $H_2$ without any clear supporting evidence that, in this case, $N_3^-$ ions scavenge the short-lived dry electrons. This is consistent with the enhanced contribution of short tracks for the higher LET tritium β-radiolysis as compared to γ radiolysis. Indeed, in this case, the short-track geometry would be competitively more favorable to the subpicosecond recombination reaction of $e_{dry}^-$ with its nearby parent water cation ($H_2O^{\bullet+}$) than to its scavenging by the homogeneously distributed $N_3^-$ ions.

A final remark should be made here regarding the origin of the small reduction that is observed, for both types of radiation, in the yields of $H_2$ with increasing azide concentration from $10^{-4}$ up to ~0.1–1 M. In fact, as shown in Fig. 4, our calculations indicate that the $H_2$ production originating from the ($H^\bullet$ + $e_{aq}^-$) reaction (1) quickly decreases as the $N_3^-$ concentration increases. This result is of course a clear signature that $N_3^-$ ions readily scavenge $H^\bullet$ atoms, thus preventing them from contributing to this reaction. By contrast, the formation of $H_2$ through the ($e_{aq}^-$ + $e_{aq}^-$) reaction (2) should in principle be rather unaffected by the presence of $N_3^-$, $N_3^-$ being highly unreactive towards $e_{aq}^-$. Actually, it is indirectly because the hydrated electrons that have not reacted with $H^\bullet$ through reaction (1) become now available to participate to reaction (2). Overall, there is a kind of compensation between the two contributions involved in the $H_2$ production, the contribution from reaction (1) dominating slightly.

# 4. Conclusions

Monte Carlo track chemistry simulations have been employed to investigate the scavengeability by azide ions ($N_3^-$) of the molecular hydrogen yield produced in water irradiated with 300 MeV protons (which mimic irradiation with $^{60}$Co γ rays or fast electrons) and tritium β-electrons at 25 °C. From this study, we clearly show that the formation of $H_2$ from $^3$H β-particles is higher than in the case of $^{60}$Co γ rays, a result that is easily explained by the difference of the structure of radiation tracks. The track structure in the case of $^{60}$Co γ irradiation is composed of well-separated (spherical) spurs, which contrasts with the short (roughly cylindrical) tracks observed in the case of higher-LET tritium β-electrons. The greater linear energy transfer of $^3$H β-electrons leads to an increased local concentration of reactants. The distance between the primary events is thus much smaller than in the tracks of $^{60}$Co γ rays. Consequently, we find more molecular products ($H_2$ in the case considered in this work) in tritium radiolysis than in γ radiolysis.

Our calculations of the $H_2$ yields from γ- and $^3$H β-radiolysis of $NaN_3$ solutions show a very good agreement with experiment over a large range of $N_3^-$ concentrations. For $^{60}$Co γ-radiolysis, however, our $H_2$ yields fail to reproduce the sharp decrease that is observed experimentally at high (>1 M) azide concentrations. These results are consistent with previous Monte Carlo simulations that suggested that such a decrease reflected the possibility that low-energy (or "dry") secondary electrons could be scavenged by $N_3^-$ prior to trapping and hydration in the subpicosecond physicochemical stage. Most interestingly, for $^3$H β-radiolysis, we do not observe any marked decrease in the molecular hydrogen yields at high $N_3^-$ concentrations as we do for γ irradiation. In other words, there is no clear evidence that, in this case, $N_3^-$ ions scavenge the short-lived dry electrons. This is consistent with the enhanced contribution of short tracks for the higher LET $^3$H β-radiolysis as compared to γ radiolysis. Indeed, the short-track geometry is competitively more favorable to the geminate recombination of $e_{dry}^-$ with their nearby parent water cations than their scavenging by the homogeneously distributed $N_3^-$ ions. In order to further examine these results, we are currently working to introduce this ultra-fast (<1 ps) capture of the dry electron into our simulation models.

In summary, this work, like our previous ones on the subject, provides a strong support for a picture of tritium β-radiolysis in terms of short tracks of high local LET.

# Conflicts of interest

There are no conflicts of interest to declare.

# Acknowledgements

S. S. is the recipient of a doctoral scholarship from the Natural Sciences and Engineering Research Council of Canada (NSERC). This work received financial assistance from Atomic Energy of Canada Limited (Contract no. RD-1.3.5.1-4511). The research of J.-P. J.-G. is supported by the NSERC Discovery Grant No. RGPIN-2015-06100.

# Notes and references

1 C. von Sonntag, *Free-Radical-Induced DNA Damage and Its Repair*, Springer-Verlag, Berlin, 2006.
2 D. R. McCracken, K. T. Tsang and P. J. Laughton, *Aspects of the physics and chemistry of water radiolysis by fast neutrons and fast electrons in nuclear reactors*, Report AECL No. 11895, Atomic Energy of Canada Limited, Chalk River, Ontario, Canada, 2009.
3 P. O'Neill and P. Wardman, *Int. J. Radiat. Biol.*, 2009, **85**, 9; P. Wardman, *Br. J. Radiol.*, 2009, **82**, 89.
4 E. I. Azzam, J.-P. Jay-Gerin and D. Pain, *Cancer Lett.*, 2012, **327**, 48.
5 J. W. T. Spinks and R. J. Woods, *An Introduction to Radiation Chemistry*, Wiley, New York, 3rd edn, 1990.
6 A. Mozumder, *Fundamentals of Radiation Chemistry*, Academic Press, San Diego, California, 1999.
7 C. Ferradini and J.-P. Jay-Gerin, *Can. J. Chem.*, 1999, **77**, 1542; see also J.-P. Jay-Gerin and C. Ferradini, in *Excess Electrons in*

*Dielectric Media*, ed. C. Ferradini and J.-P. Jay-Gerin, CRC Press, Boca Raton, Florida, 1991, p. 259.

8 J. A. LaVerne, *Radiat. Res.*, 2000, **153**, 487.

9 G. V. Buxton, in *Charged Particle and Photon Interactions with Matter: Chemical, Physicochemical, and Biological Consequences with Applications*, ed. A. Mozumder and Y. Hatano, Marcel Dekker, New York, 2004, p. 331.

10 Y. Muroya, I. Plante, E. I. Azzam, J. Meesungnoen, Y. Katsumura and J.-P. Jay-Gerin, *Radiat. Res.*, 2006, **165**, 485.

11 J. Meesungnoen and J.-P. Jay-Gerin, in *Charged Particle and Photon Interactions with Matter. Recent Advances, Applications, and Interfaces*, ed. Y. Hatano, Y. Katsumura and A. Mozumder, Taylor & Francis Group, Boca Raton, Florida, 2011, p. 355; see also J. Meesungnoen, Ph.D. thesis, Université de Sherbrooke, Sherbrooke, Québec, Canada, 2007.

12 A. J. Elliot and D. M. Bartels, *The reaction set, rate constants and g-values for the simulation of the radiolysis of light water over the range 20 to 350 °C based on information available in 2008*, Report AECL No. 153-127160-450-001, Atomic Energy of Canada Limited, Chalk River, Ontario, Canada, 2009.

13 V. Kanike, J. Meesungnoen and J.-P. Jay-Gerin, *RSC Adv.*, 2015, **5**, 43361.

14 J. L. Magee, *Annu. Rev. Nucl. Sci.*, 1953, **3**, 171.

15 G. R. Freeman, in *Proceedings of the Workshop on the Interface between Radiation Chemistry and Radiation Physics*, Report ANL-82-88, ed. M. A. Dillon, R. J. Hanrahan, R. Holroyd, Y.-K. Kim, M. C. Sauer Jr and L. H. Toburen, Argonne National Laboratory, Argonne, Illinois, 1983, p. 9.

16 Hydrogen-3 or tritium ($^3$H) is a radioactive isotope of hydrogen. Its nucleus consists of a proton and two neutrons. The most common chemical form of tritium is tritium oxide, also called "tritiated water" (usually represented as $^3$HOH). As it decays, $^3$H emits ionizing radiation in the form of β-electrons with the following characteristics: maximum kinetic energy: ∼18.6 keV, mean kinetic energy released: ∼5.7 keV, "mean energy of energy deposition" in water: ∼7.8 keV, maximum range in water at 25 °C: ∼5.5 μm (∼6 mm in air). The mean (averaged over whole track) LET of $^3$H β-electrons in water (∼5.9 eV nm$^{-1}$) is ∼20 times greater than that of the Compton electrons (∼1 MeV) generated by $^{60}$Co γ-rays (∼0.3 eV nm$^{-1}$).

17 D. E. Watt, *Quantities for Dosimetry of Ionizing Radiations in Liquid Water*, Taylor & Francis, London, 1996.

18 L. Mirsaleh Kohan, S. Sanguanmith, J. Meesungnoen, P. Causey, C. R. Stuart and J.-P. Jay-Gerin, *RSC Adv.*, 2013, **3**, 19282.

19 A. Mozumder and J. L. Magee, *J. Chem. Phys.*, 1966, **45**, 3332; A. Mozumder and J. L. Magee, *Radiat. Res.*, 1966, **28**, 203.

20 Throughout this paper, radiation chemical yields are quoted in units of molecules per 100 eV, as $g(X)$ for primary (or "escape") yields and $G(X)$ for experimentally measured yields. Recall here briefly that the so-called "primary" radical and molecular yields are defined as the numbers of species formed or destroyed per 100 eV of absorbed energy that remain after spurs/tracks have dissipated and become available to react with added solutes (if any) at moderate concentrations. For conversion into SI units (mol J$^{-1}$), 1 molecule per 100 eV ≈ 0.10364 μmol J$^{-1}$.

21 A. Appleby and W. F. Gagnon, *J. Phys. Chem.*, 1971, **75**, 601.

22 W. F. Gagnon and A. Appleby, *Scavenger studies in tritiated water*, Paper of the Journal Series, New Jersey Agricultural Experimental Station, Rutgers University, Department of Environmental Sciences, New Brunswick, New Jersey, 1971.

23 G. Lemaire, C. Ferradini and J. Pucheault, *J. Phys. Chem.*, 1972, **76**, 1542; see also G. Lemaire and C. Ferradini, *Radiochem. Radioanal. Lett.*, 1970, **5**, 175; G. Lemaire and C. Ferradini, in *Proceedings of the Third Tihany Symposium on Radiation Chemistry*, ed. J. Dobó and P. Hedvig, Akadémiai Kiadó, Budapest, 1972, vol. 2, p. 1213.

24 W. F. Gagnon and A. Appleby, in *Tritium*, ed. A. A. Moghissi and M. W. Carter, Messenger Graphics, Phoenix, Arizona, 1973, p. 192.

25 E. A. Christman, Ph.D. thesis, Rutgers University, New Brunswick, New Jersey, 1977.

26 R. E. Harris and S. M. Pimblott, *Radiat. Res.*, 2002, **158**, 493.

27 S. L. Butarbutar, S. Sanguanmith, J. Meesungnoen, P. Causey, C. R. Stuart and J.-P. Jay-Gerin, *RSC Adv.*, 2014, **4**, 22980.

28 S. Mustaree, J. Meesungnoen, S. L. Butarbutar, P. Causey, C. R. Stuart and J.-P. Jay-Gerin, *RSC Adv.*, 2014, **4**, 43572.

29 T. J. Hardwick, *Discuss. Faraday Soc.*, 1952, **12**, 203; see also A. O. Allen, *Radiat. Res.*, 1954, **1**, 85.

30 E. J. Hart, *Radiat. Res.*, 1954, **1**, 53; see also W. R. McDonell and E. J. Hart, *J. Am. Chem. Soc.*, 1954, **76**, 2121.

31 E. Collinson, F. S. Dainton and J. Kroh, *Proc. R. Soc. London, Ser. A*, 1962, **265**, 422; see also E. Collinson, F. S. Dainton and J. Kroh, *Nature*, 1960, **187**, 475 these same authors (E. Collinson, F. S. Dainton and J. Kroh, *Proc. R. Soc. London, Ser. A*, 1962, **265**, 430) also described and discussed the isotope effects observed for irradiations of 0.05 M sulfuric acid solutions with 1.6 and 3 MeV α-particles and tritium β-particles.

32 R. Bensasson, A. Bernas, M. Bodard, L. Bouby, M. Cottin, M. Duflo, F. Kieffer, A. Koulkès, N. Leray, J. Pucheault and C. Vermeil, in *Tables of Constants and Numerical Data*, ed. M. Haïssinsky and M. Magat, Pergamon, Oxford, 1963, vol. 13, p. 15.

33 In liquid water at 25 °C, time-resolved femtosecond laser spectroscopic experiments have revealed that electron "localization" and "hydration" occur in quick succession on time scales of ∼50–300 fs and ∼240 fs to 1 ps, respectively (see, for example, C.-R. Wang, T. Luo and Q.-B. Lu, *Phys. Chem. Chem. Phys.*, 2008, **10**, 4463). Monte Carlo simulations of the thermalization of $e_{sub}^-$ in solid water have shown that thermalization times vary from ∼3 to 182 fs when the initial electron energy changes from 0.35 to 7.2 eV, respectively, with an estimated average value of ∼60 fs; see T. Goulet, J. P. Patau and J.-P. Jay-Gerin, *J. Phys. Chem.*, 1990, **94**, 7312.

34 J. Meesungnoen, S. Sanguanmith and J.-P. Jay-Gerin, *RSC Adv.*, 2015, **5**, 76813.

35 M. Sterniczuk and D. M. Bartels, *J. Phys. Chem. A*, 2016, **120**, 200; see also G. P. Horne, S. M. Pimblott and J. A. LaVerne, *J. Phys. Chem. B*, 2017, **121**, 5385.

 

36 The secondary (or "dry") electron released in the ionization event can cause further ionization and excitation to occur if it has sufficient kinetic energy. Eventually, its energy falls below the first electronic excitation threshold of water (~7.3 eV in amorphous ice at 14 K, see: M. Michaud, P. Cloutier and L. Sanche, *Phys. Rev. A*, 1991, **44**, 5624), forming the so-called "sub-excitation electron" (R. L. Platzman, *Radiat. Res.*, 1955, **2**, 1). The latter loses the rest of its energy relatively slowly by exciting vibrational and rotational modes of water molecules. Once it is thermalized ($e_{th}^-$), it can get localized or "trapped" ($e_{tr}^-$) in a pre-existing potential energy well of appropriate depth in the liquid before it reaches a fully relaxed, hydrated state ($e_{aq}^-$) as the dipoles of the surrounding molecules orient under the influence of the negative charge of the electron. The trapped (or "wet") electron has sometimes been called "incompletely relaxed" or "prehydrated" electron in the literature (G. R. Freeman, in *Kinetics of Nonhomogeneous Processes*, ed. G. R. Freeman, Wiley, New York, 1987, p. 19).
37 H. Schwarz, *J. Phys. Chem.*, 1969, **73**, 1928.
38 B. Pastina, J. A. LaVerne and S. M. Pimblott, *J. Phys. Chem. A*, 1999, **103**, 5841.
39 V. Cobut, J.-P. Jay-Gerin, Y. Frongillo and J. P. Patau, *Radiat. Phys. Chem.*, 1996, **47**, 247.
40 M.-A. Hervé du Penhoat, T. Goulet, Y. Frongillo, M.-J. Fraser, P. Bernat and J.-P. Jay-Gerin, *J. Phys. Chem. A*, 2000, **104**, 11757.
41 D. M. Bartels, J. Henshaw and H. E. Sims, *Radiat. Phys. Chem.*, 2013, **82**, 16; K. Kanjana, K. S. Haygarth, W. Wu and D. M. Bartels, *Radiat. Phys. Chem.*, 2013, **82**, 25.
42 C. D. Alcorn, J.-C. Brodovitch, P. W. Percival, M. Smith and K. Ghandi, *Chem. Phys.*, 2014, **435**, 29.
43 A. Kuppermann, in *Actions Chimiques et Biologiques des Radiations*, ed. M. Haïssinsky, Tome 5, Masson, Paris, 1961, p. 85.
44 V. Cobut, Y. Frongillo, J. P. Patau, T. Goulet, M.-J. Fraser and J.-P. Jay-Gerin, *Radiat. Phys. Chem.*, 1998, **51**, 229.
45 Y. Frongillo, T. Goulet, M.-J. Fraser, V. Cobut, J. P. Patau and J.-P. Jay-Gerin, *Radiat. Phys. Chem.*, 1998, **51**, 245.
46 R. Meesat, S. Sanguanmith, J. Meesungnoen, M. Lepage, A. Khalil and J.-P. Jay-Gerin, *Radiat. Res.*, 2012, **177**, 813.
47 R. L. Platzman, in *Radiation Biology and Medicine. Selected Reviews in the Life Sciences*, ed. W. D. Claus, Addison-Wesley, Reading, Massachusetts, 1958, p. 15. See also; A. Kuppermann, *J. Chem. Educ.*, 1959, **36**, 279.
48 S. Sanguanmith, J. Meesungnoen, Y. Muroya, M. Lin, Y. Katsumura and J.-P. Jay-Gerin, *Phys. Chem. Chem. Phys.*, 2012, **14**, 16731.
49 M. Tachiya, *Radiat. Phys. Chem.*, 1983, **21**, 167.
50 S. M. Pimblott, M. J. Pilling and N. J. B. Green, *Radiat. Phys. Chem.*, 1991, **37**, 377; see also S. M. Pimblott and N. J. B. Green, in *Research in Chemical Kinetics*, ed. R. G. Compton and G. Hancock, Elsevier, Amsterdam, 1995, vol. 3, p. 117.
51 T. Goulet, M.-J. Fraser, Y. Frongillo and J.-P. Jay-Gerin, *Radiat. Phys. Chem.*, 1998, **51**, 85.
52 I. Plante, Ph.D. thesis, Université de Sherbrooke, Sherbrooke, Québec, Canada, 2009.
53 T. Tippayamontri, S. Sanguanmith, J. Meesungnoen, G. R. Sunaryo and J.-P. Jay-Gerin, in *Recent Research Developments in Physical Chemistry*, ed. S. G. Pandalai, Transworld Research Network, Trivandrum, Kerala, India, 2009, vol. 10, p. 143.
54 *CRC Handbook of Chemistry and Physics*, ed. D. R. Lide, CRC Press, Boca Raton, Florida, 84th edn, 2003.
55 Except for the peculiar bimolecular self-recombination of $e_{aq}^-$ for which there is no experimental evidence of any ionic strength effect (see K. H. Schmidt and D. M. Bartels, *Chem. Phys.*, 1995, **190**, 145).
56 S. Sanguanmith, Y. Muroya, T. Tippayamontri, J. Meesungnoen, M. Lin, Y. Katsumura and J.-P. Jay-Gerin, *Phys. Chem. Chem. Phys.*, 2011, **13**, 10690.
57 R. E. Weston Jr and H. A. Schwarz, *Chemical Kinetics*, Prentice-Hall, Englewood Cliffs, New Jersey, 1972.
58 ICRU Report 17, *Radiation Dosimetry: X Rays Generated at Potentials of 5 to 150 kV*, International Commission on Radiation Units and Measurements, Washington, D.C., 1970. See also J. Law, *Phys. Med. Biol.*, 1969, **14**, 607.
59 S. Heinze, T. Stolz, D. Ducret and J.-C. Colson, *Fusion Sci. Technol.*, 2005, **48**, 673.
60 E. Peled, U. Mirski and G. Czapski, *J. Phys. Chem.*, 1971, **75**, 31. Note that these authors used a $^{137}$Cs $\gamma$ source for their irradiations.
61 M. Ye, K. P. Madden, R. W. Fessenden and R. H. Schuler, *J. Phys. Chem.*, 1986, **90**, 5397.
62 G. V. Buxton, C. L. Greenstock, W. P. Helman and A. B. Ross, *J. Phys. Chem. Ref. Data*, 1988, **17**, 513.
63 S. P. Mezyk and D. M. Bartels, *J. Phys. Chem. A*, 2005, **109**, 11823.
64 Z. B. Alfassi and R. H. Schuler, *J. Phys. Chem.*, 1985, **89**, 3359; Z. B. Alfassi, W. A. Prütz and R. H. Schuler, *J. Phys. Chem.*, 1986, **90**, 1198.
65 E. Hayon and M. Simic, *J. Am. Chem. Soc.*, 1970, **92**, 7486.
66 T. E. Eriksen, J. Lind and G. Merényi, *Radiochem. Radioanal. Lett.*, 1981, **48**, 405.
67 T. Ichino and R. W. Fessenden, *J. Phys. Chem. A*, 2007, **111**, 2527.
68 A. Singh, G. W. Koroll and R. B. Cundall, *Radiat. Phys. Chem.*, 1982, **19**, 137.
69 G. R. Dey, *Res. Chem. Intermed.*, 2007, **33**, 599.
70 P. Neta, R. E. Huie and A. B. Ross, *J. Phys. Chem. Ref. Data*, 1988, **17**, 1027.
71 X. Liu, M. A. MacDonald and R. D. Coombe, *J. Phys. Chem.*, 1992, **96**, 4907.
72 The product of a solute's (or scavenger's) concentration and its rate constant for reaction with one of the primary radical species is called its "scavenging power", with units of $s^{-1}$. The inverse of the scavenging power gives a measure of the time scale over which the scavenging is occurring or, in other words, the lifetime of the radical with respect to that reaction (see ref. 2).

73 For example, in the presence of 5 M $N_3^-$, the measured yield of $H_2$ is decreased to almost one-third of its value in the absence of azide (see ref. 60).

74 See also S. M. Pimblott and J. A. LaVerne, *J. Phys. Chem.*, 1998, **102**, 2967.

75 This relatively large dispersion of experimental data is probably explained by the fact that experiments are difficult to perform with $^3H$ as the source of β-particle radiation. Contrary to γ-irradiation studies, the irradiation cannot be stopped and hence estimation of the dose given to the sample is susceptible to significant error (see ref. 26).